(9) F. H. Nielson and D. A. Allerich, *Fed. Proc., Fed. Am. Soc. Exp. Biol.*, **33**, 1767 (1974).
(10) G. Hammes and M. Morrell, *J. Am. Chem. Soc.*, **86**, 1497 (1964).
(11) $Q \equiv [K_a(ML) + (K_M + H)K_a(1 + \alpha) \pm HL(2K_M \pm H)]/[ML(K_a \pm H) + (K_M \pm H)((K_a + H)(1 + \alpha) + HL)]$; $R = [ML(K_a + 2H) \pm H((K_a + H)(1 + \alpha) + HL)]/[ML(K_a + H) + (K_M + H)[(K_a + H)(1 + \alpha) + HL)]$; $\alpha = \ln/(K_{In} + H)$; $K_M = K_{ML}/(K_{MHL}K_a)$. For NiHP$_3O_{10}$ Q ranged from 0.7 to 1.0 and R from 0.9 to 1.3; for NiHP$_2$O$_7$, $Q \sim 0.9$ to 1.2, $R \sim 0.8$ to 1.2.
(12) M. Eigen and K. Tamm, *Z. Elektrochem.*, **66**, 93, 107 (1962).
(13) J. W. Neely and R. E. Connick, *J. Am. Chem. Soc.*, **94**, 3419 (1972).
(14) The earlier kinetic measurements of NiHP$_3$O$_{10}$ and NiHP$_2$O$_7$ were carried out in 0.1 M tetramethylammonium chloride. TMA$^+$ binds much less, if at all, to the phosphate moiety; therefore k_{lp} values for these two systems must be calculated with a value of K_{os}' which includes only ionic strength adjustments, and not corrections for the binding of the cation of the supporting electrolyte. K_{os}' can be estimated to be 70 and 300 for the di- and triphosphate, respectively. Since the value for k_{12} involves K_{os}' ($k_{12} = K_{os}' k_{lp}$) the forward rate constants for the two different studies of the complexation of nickel with pyro- and tripolyphosphate will reflect the influence of the supporting electrolyte, i.e., k_{12}(TMACl) $> k_{12}$(KNO$_3$).
(15) The rate constants in Table III differ slightly from those tabulated in an earlier review (ref 4).
(16) T. A. Glassman, C. Cooper, L. W. Harrison, and T. J. Swift, *Biochemistry*, **10**, 843 (1971).

Interactions of Divalent Metal Ions with Inorganic and Nucleoside Phosphates. 6. A Thermodynamic and Kinetic Study of the Nickel(II)–Adenosine 5'-Triphosphate and –Adenosine 5'-Diphosphate Systems

Cheryl Miller Frey and John E. Stuehr*[2]

Contribution from the Department of Chemistry, Case Western Reserve University, Cleveland, Ohio 44106. Received August 13, 1976

Abstract: Equilibrium binding and relaxation kinetic data are presented for the interactions of Ni(II) with ADP and ATP. Spectral measurements indicate the formation of Ni$_2$L complexes with both nucleotides; $K_{Ni_2L} = 40$ and 250 M^{-1} for ADP and ATP, respectively, at 15 °C and $I = 0.1$. Temperature-jump relaxation experiments, carried out over wide ranges of concentrations, were consistent with a three-step mechanism involving the formation of two 1:1 complexes (involving the phosphate moiety and phosphate plus base, respectively) and a 2:1 complex. Rate constants for the formation of the phosphate and the Ni$_2$L complexes were found to be similar to those for the corresponding cytosine and inorganic phosphate systems in which analogous complexes were formed. Formation of the back-bound 1:1 complex was characterized by rate constants of 450 and 1000 s^{-1} for the NiADP and NiATP systems.

A large number of enzymes require metal ions for activation, especially enzymes which utilize adenine nucleotides as cofactors.[3] In such instances there is substantial evidence that the substrate is the metal–nucleotide complex and not the free nucleotide.[4] As a consequence, considerable effort has gone into characterizing the nature of the interactions between metal ions and adenine nucleotides. Within the last decade there have been a number of studies[5]—via temperature jump spectrometry,[6,7] NMR,[8–10] UV spectroscopy,[11] and ORD[12]—of transition metal binding to ATP. The conclusions of these studies have been in disagreement with respect to both the duration and the site(s) of the metal–nucleotide interactions.

The major binding sites of Ni(II) with ATP are the phosphate oxygens. Using ^{31}P NMR, Cohn and Hughes[8] and Sternlicht et al.[9] have shown that nickel binds to all three phosphate oxygens in the ML complex. They also found that the proton signals of the adenine ring were extensively broadened upon addition of Ni(II) to an aqueous (D$_2$O) solution of ATP ($\sim$0.1 M). From the temperature dependences of the broadening of the proton and phosphorus signals, Sternlicht et al. were able to show that the lifetimes of the metal ion in the vicinity of both the ring and the phosphate backbone were virtually identical. They concluded that in the 1:1 complex the nickel ion was bound simultaneously to the phosphate oxygens and the N$_7$ position in ATP.

The first temperature-jump studies of complex formation with nickel and ATP were in dilute solution ($\sim$5 × 10^{-4} M) and were characterized by rate constants that depended on only the charge type of the ligand and the water exchange rate of the metal ion.[6] However, the dissociation rate constant obtained from this study was about 30 times faster than the dissociation rate obtained by Sternlicht et al.[9b] in their NMR study of Ni(II)–ATP. In order to resolve this discrepancy between temperature-jump and NMR results, Hammes and Miller[7] reinvestigated the relaxation spectra of a number of metal ions, including Ni(II), with ATP, this time at high concentrations (0.01–0.1 M) of both metal and ligand. From extrapolation of their earlier low concentration rate data, they assumed that the previously studied time would be too fast to be observed at these high concentrations. For Ni(II)–ATP two times were observed. One time was concentration and pH *dependent* and was attributed to polynuclear complex formation. The second time was concentration *independent*, suggesting that the process was intramolecular. One likely possibility was thought to be the opening and closing of a backbound (ML') complex as represented mechanistically in Table I. Schematic representations of the 1:1 complexes are shown in Figure 1.

More recently, our studies of the complexation of Mg(II) with CTP, CDP, ATP, and ADP[13] and Ni(II) with CTP and CDP[14] have shown that the kinetic profiles obtained in these systems could be quantitatively accounted for by a mechanism involving the formation of ML and M$_2$L complexes (Table I). This is particularly relevant to the present study because the formation of an M$_2$L complex between nickel and ATP has been observed.[15] Thus we are in the position of having not only a multiplicity of possible mechanisms, but also a multiplicity of complexes to consider in our analysis of the kinetic data for Ni(II)–ATP and Ni(II)–ADP. For a detailed discussion of these and other proposed mechanisms, the reader is referred to a recent review.[16]

We have taken several steps to maximize the amount of

Table I. Summary of Mechanisms Proposed for the Interactions of Various Divalent Metal Ions with Adenine Nucleotides[a]

Mechanism	Systems	Technique	Ref
(1) $M + L \rightleftharpoons ML \rightleftharpoons ML'$	Ni–ATP, Co–ATP	T-jump	7
	Mn–ATP	NMR	10
(2) $\begin{matrix} M + 2L \rightleftharpoons ML + L \\ \| \qquad\qquad \| \\ M + L_2 \rightleftharpoons ML_2 \end{matrix}$	Ni–ATP, Co–ATP, Mn–ATP	NMR, T-jump	22
(3) $2M + L \rightleftharpoons ML + M \rightleftharpoons M_2L$ Mg–ATP, Mg–ADP		T-jump	13

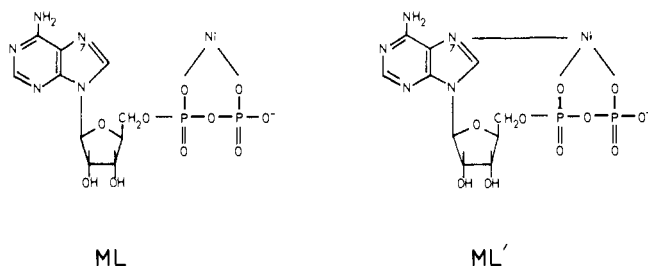[a] None of these mechanisms fit the present data; see text.

Figure 1. Structures of the 1:1 phosphate-bound (ML) and N_7-ring-bound (ML') complexes for NiADP. The complexes M_2L and M_2L' are the complexes to which a second metal ion has coordinated.

information available to us. First, kinetic data for both systems were taken over a continuous wide concentration range such that the measurements encompassed and bridged the ranges covered in the earlier low concentration temperature-jump work and the later high concentration NMR and temperature-jump studs. Second, spectral measurements were made to determine K_{M_2L} values for Ni_2ATP and Ni_2ADP under the conditions of our kinetic experiments. Third, we had previously redetermined the metal ion binding constants relevant to this study with particular attention to whether bis as well as mono complexes were being formed.[17] Fourth, our previous work on the kinetics of Ni(II) with the inorganic phosphates and cytosine nucleotides has established rate constants for metal complexation with the phosphate moieties alone.[14] Finally, we can obtain a quantitative measure of the stability of the proposed back-bound complex, ML', from the increase in stability constants for the adenine nucleotides compared to the inorganic phosphates. As a result, we now have considerable mechanistic and thermodynamic information which can be brought to bear upon our analysis of the kinetics of the Ni(II)–ADP and Ni(II)–ATP systems.

Experimental Section

Materials and Methods. All compounds used in the kinetic and spectral measurements were prepared or purchased as described earlier.[13] Supporting electrolyte for the kinetic work was 0.1 M KNO_3, while 0.1 M KCl was used for the difference spectra. Spectral measurements and temperature-jump relaxation data were obtained at 15 °C as described in the previous paper.[14]

Treatment of Data. In the previous study[14] we used a spectral technique[15] to obtain the stability constants for the M_2L complex formed with nickel and cytosine nucleotides (CTP, CDP). In Figure 2 we can see that the difference spectra for nickel with ATP or ADP are rather large (~0.10 absorbance unit) even at metal–ligand ratios of 1:1. This has been interpreted as due to the formation of a complex (ML') involving back-bonding to a nitrogen on the adenine ring system. The composition of the solutions in the two cuvettes can be described as follows:

cell 1 (metal + nucleotide)

$$A_1 = \epsilon_L(L) + \epsilon_{ML}(ML) + \epsilon_{ML'}(ML') + \epsilon_{M_2L}(M_2L) \qquad (1)$$

and cell 2 (nucleotide alone, L^0 = total concentration of nucleotide)

Table II. Equilibrium Constants for Metal Complex and Ligand Ionization Equilibria in 0.1 M KNO_3 at 15 °C[a]

Ligand	pK_1	pK_2	System	Log K_{MHL}	Log K_{ML}[c]	K_{M_2L}[b]
ATP	4.18	6.57	Ni–ATP	2.78	4.79	250 ± 50
ADP	4.05	6.41	Ni–ADP	2.30	4.18	40 ± 20

[a] All data from ref 17 unless otherwise indicated. [b] Present measurements; see text. [c] K_Σ values; see eq 5.

$$A_2 = \epsilon_L(L^0) \qquad (2)$$

We have chosen our experimental conditions (pH >6) so that protonated complexes such as MHL can be neglected. In addition, we assume that $\epsilon_{ML} = \epsilon_L$, i.e., chelation of the metal ion to only the phosphate backbone does not affect the ring spectrum.[18] Under experimental conditions such that $M^0 \gg L^0$ (so that $M \simeq M^0$), and with the following definitions:

$$K_{ML} = ML/(M \cdot L) \quad K_{M_2L} = M_2L/(ML \cdot M) \quad K_{ML'} = ML'/ML$$
$$(3)$$

the observed difference in absorbance is simply[15]

$$\frac{1}{\Delta A} = \frac{\left[\dfrac{1 + K_{ML'}}{M^0} + K_{M_2L} \right]}{\Delta\epsilon_{ML'}K_{ML'}L^0/M^0 + \Delta\epsilon_{M_2L}K_{M_2L}L^0} \qquad (4)$$

where $\Delta\epsilon$ represents the difference in extinction coefficient between the species indicated and free ligand. As $1/M^0 \rightarrow 0$, $1/\Delta A \rightarrow K_{M_2L}/(\Delta\epsilon_{M_2L}L^0)$. Conversely, as $1/\Delta A \rightarrow 0$, $1/M^0 \rightarrow (-K_{M_2l})/(1 + K_{ML'})$.

In the treatment of data, we shall need to know the constants for the formation of the back-bound complex ML' for both Ni(II)–ADP nad Ni(II)–ATP. We can obtain these values as follows. For the reaction
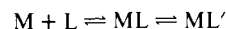
$$M + L \rightleftharpoons ML \rightleftharpoons ML'$$

the overall measured equilibrium constant is

$$K_\Sigma = \frac{[ML + ML']}{[M][L]} = K_{ML}[1 + K_{ML'}] \qquad (5)$$

where K_{ML} and $K_{ML'}$ are defined in eq 3. Therefore, if a system is known where only the phosphate-bound complex is formed ($NiHP_2O_7$, $NiHP_3O_{10}$), a value for K_{ML} is known and $K_{ML'}$ can be estimated from eq 5. From our measurements of the stability constants[17] of the appropriate nucleotides and phosphates, under identical conditions of temperature, ionic strength, and supporting electrolyte, we compute $K_{ML'} = 1.5$ and 3.8 for Ni(II)–ATP and Ni(II)–ADP, respectively.

All experimental relaxation times in Table III were computed from a minimum of three oscilloscope traces. The various equilibrium constants used to calculate the concentrations of individual species can be found in Table II. All calculations were carried out on a Univac 1108 computer.

Results

Spectral Measurements. Figure 2 shows the difference spectra of Ni(II)–ADP and Ni(II)–ATP. The difference spectra are similar in morphology to those observed by Happe

Table III. Kinetic Data at 15 °C, 0.1 M KNO_3

M^0, M × 10²	L^0, M × 10²	pH	$1/\tau$ (exptl), s⁻¹	$1/\tau$ (calcd), s⁻¹
			1. NiATP	
8.81	9.05	5.63	1118	1263
7.05	7.24	5.94	1225	1015
3.53	3.62	6.01	924	953
2.92	2.98	6.26	1024	855
2.04	2.09	6.40	891	795
1.45	1.52	6.47	746	739
1.46	1.49	6.43	750	769
1.02	1.06	6.32	673	733
0.872	0.909	6.23	628	730
0.727	0.758	6.12	498	734
0.485	0.498	6.67	528	605
0.242	0.249	6.46	410	495
0.092	0.095	6.72	315	321
0.058	0.059	6.47	251	267
			2. NiADP	
4.65	5.00	6.01	509	485
2.94	3.92	6.03	500	466
2.35	3.14	6.13	482	465
2.33	2.50	6.16	413	457
1.65	2.20	6.17	452	450
1.90	1.96	5.85	422	490
1.52	1.57	5.87	478	476
1.00	1.00	6.54	423	413
0.980	1.00	6.19	452	423
0.980	1.00	6.57	430	407
0.882	0.902	6.32	324	407
0.720	0.750	6.54	358	381
0.706	0.722	6.33	341	389
0.540	0.560	6.50	333	357
0.270	0.280	6.62	255	288
0.052	0.054	6.56	107	146

[a] Kinetic data obtained with 4–8 × 10⁻⁵ M chlorophenol red indicator. [b] Overall concentrations. [c] a_H values converted to C_H by γ_H = 0.83. [d] Typically ±5% deviation in average of at least three traces. [e] Slowest root from eq 6.

Figure 2. Differential UV absorption spectra at 15 °C for Ni^{2+} with ADP and ATP. Overall concentrations: 1×10^{-4} M Ni^{2+}, 1×10^{-4} M nucleotides, at pH 6.6. Medium: 0.1 M KCl.

Figure 3. $1/\Delta A$ vs. $1/M^0$ for the Ni^{2+}–ATP system at 15 °C, $I = 0.1$, and pH 6.6. The concentration of ATP was 1×10^{-4} M; that of Ni^{2+} varied from 0.01 to 0.025 M.

and Ward[19] for ADP complexes with Zn(II), Mn(II), and Mg(II).

Plots of $1/\Delta A$ vs. $1/M^0$ (Figure 3) are similar to those observed with the cytosine series[14] except that there is now less scatter because of the larger absorbance differences. Table II contains the values obtained for K_{M_2L}. The uncertainties reflect the effects of a rather long extrapolation to obtain the composite constant $(-K_{M_2L})(1 + K_{ML'})$. Our value of 250 for K_{M_2L} for Ni_2ATP at 15 °C is the same as that determined by Glassman et al.[15] at 25 °C.

In order to see if there was any evidence for an interaction between Ni(II) and adenosine itself, difference spectra were run from 230 to 300 nm. A very small difference (±0.005 absorbance unit) was observed. We concluded that the stability constant for the Ni(II)–adenosine interaction is at least an order of magnitude less than that for the Ni(II)–ATP system.[20]

Kinetic Data. The kinetics of the complexation of nickel with ADP^{3-} and ATP^{4-} were studied at 15 °C and 0.1 M KNO_3 at metal–ligand ratios of approximately 1:1. The concentration ranges studied were typically 5×10^{-4} to 10^{-2} M, with measurements in Ni(II)–ATP extending to nearly 0.1 M. Tabulation of concentration data and relaxation times for both systems is given in Table III. The measured relaxation times are estimated to be reliable to ±5% in dilute solutions (M^0, L^0 $\simeq 10^{-3}$ M) and ±10% in more concentrated solutions where the observed relaxation effects were smaller.[21] Kinetic data for both systems in terms of $1/\tau$ vs. the concentration function
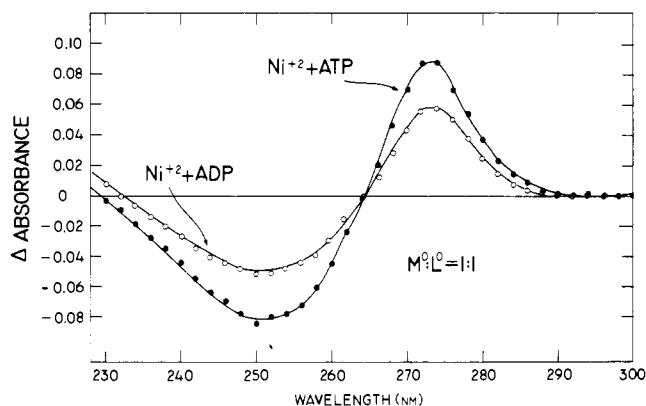
$f(C)[\equiv (M/(1 + \beta) + L)]$ (see eq 7 for definitions of symbols) for the reaction $M + L \rightleftharpoons ML$ are displayed in Figures 4 and 5. Lines or curves representing "best fit" of the experimental points[14] for the analogous inorganic phosphate and cytosine nucleotide systems are also drawn in for comparison.

For Ni(II)–ATP, the complexation kinetics have also been studied by temperature jump in both dilute and concentrated solutions by Hammes and co-workers.[6,7] Their data at low concentrations (25 °C, 0.1 M KNO_2) are in agreement with ours when the difference in temperature is allowed for. At high concentrations (~0.1 M), Hammes and Miller reported a concentration-independent time of 0.3–0.6 ms (τ^{-1} = 1500–3000), which corresponds to the plateau region we show in Figure 4. Because they did not study the intermediate concentration region, they felt that the high and low concentration data represented two different times, and hence, two different processes. Our data over the entire concentration range show that there is a smooth transition from relaxation times observed at low and high concentrations.

Figures 4 and 5 also show the kinetic behavior of the Ni(II)–ADP and Ni(II)–ATP systems compared with that of the analogous inorganic phosphate and cytosine nucleotides. A number of differences are immediately apparent. First, in neither the di- or triphosphate adenine systems do the limiting slopes (as $f(C) \rightarrow 0$) superimpose upon the corresponding cytosine or inorganic phosphate data. Second, the intercepts are lower, i.e., k_r is reduced for Ni(II)–ATP and –ADP, compared to the other compounds. And third, data for the adenine nucleotides deviate from linearity at high concentra-
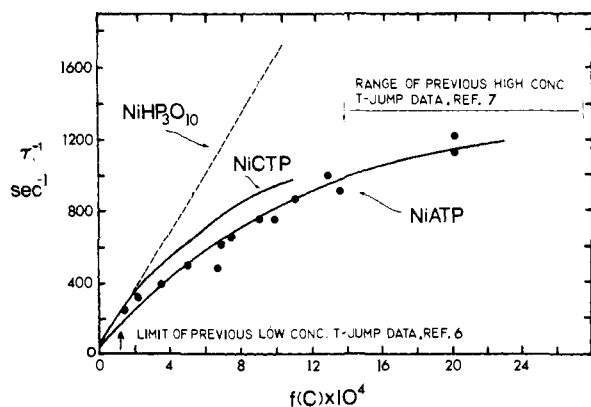
Figure 4. Dependence of $1/\tau$ upon the concentration function $f(C) \approx M/(1 + \beta) + L$ for the Ni–ATP system at 15 °C and $I = 0.1$.

Figure 5. Dependence of $1/\tau$ upon the concentration function $f(C)$ for the Ni–ATP system at 15 °C and $I = 0.1$.

tions, but do not superimpose upon data for the cytosine systems, which also deviate from linearity at about the same $f(C)$. This behavior of the nickel–adenine nucleotides is very different from the kinetic pattern displayed in our previous study of magnesium complexation,[13] where the kinetic profile was identical for the CDP, ADP, CTP, and ATP systems. Thus it is necessary to find a mechanism that not only quantitatively accounts for all the above characteristics but is also consistent with what we know about the species present in Ni(II)–ADP and Ni(II)–ATP solutions.

It is well known that a variety of two-step mechanisms can generate the observed morphology, viz., a relaxation time root that increases linearly at low concentratons and plateaus at high concentrations. The mechanisms listed in Table I have all been previously proposed to describe the complexation of various metal ions with adenine nucleotides. All three of these mechanisms can, under certain conditions, generate the desired $1/\tau$ profile.

Since we now have available a large amount of information concerning not only rates of nickel–phosphate chelation and M_2L formation from our previous studies[14] but also stability constants under the conditions of our kinetic experiments,[17] we are able to establish certain criteria with which any mechanism must be consistent. They are as follows: (1) For a given charge type the rate of *metal–phosphate* complexation must be comparable to that obtained for the Ni(II)–inorganic phosphates and the Ni(II)–cytosine nucleotides. (2) For any subsequent complexation (e.g., formation of M_2L or ML_2) the rate constants should be consistent, again dependent on charge, with the water exchange rate for nickel. (3) Those stability constants which are permuted to optimize fit must remain within experimentally determined limits. (4) It should not be necessary to invoke different mechanisms for the diphosphates vs. the triphosphates (cf. our previous kinetic experience with Mg(II) and Ni(II) nucleotide systems). Using these criteria, we tested the three mechanisms previously proposed for a fit to our experimental data. Rate constants and some stability constants (those which were not known precisely) were allowed to vary such that the best curves through the points were obtained. The following is a summary of our testing of these mechanisms.

The first mechanism we evaluated was that designated as 2 in Table I. We concluded that this mechanism was not consistent with the data for either Ni(II)–ATP or Ni(II)–ADP, for three reasons: results at different L^0/M^0 ratios were not internally consistent; rate constants for the formation of the 1:1 *phosphate-bound* complex were nearly 40% lower than values we had previously obtained[14] for similar nickel systems; and rate constants needed for the formation of the bis complexes were unusually large considering the unfavorable charge
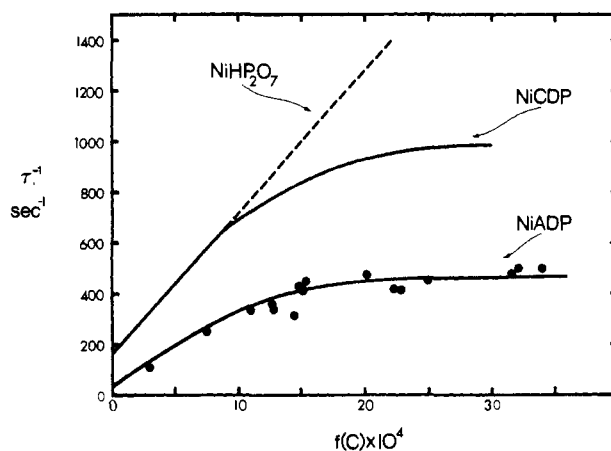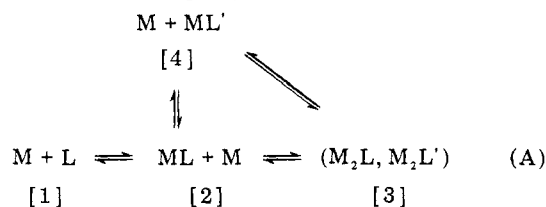
interactions involved. The next mechanism we tried was that proposed by Hammes and Miller,[7] number 1 in Table I, where the complexed species are ML and ML′. Since we have firm values for K_{ML} and $K_{ML'}$, we permuted only the two rate constants k_{12} and k_{23}. We could not obtain a quantitative fit for ATP under any conditions: the calculated data points plateaued too rapidly and could not be made to reproduce the observed concentration profile.

The third mechanism listed in Table I is the mechanism we employed in our study of the kinetics of Mg(II) with adenine and cytosine nucleotides[13] and Ni(II) with cytosine nucleotides.[14] This mechanism could not be made to reproduce the data for either ADP or ATP.

Using the criteria outlined earlier, we next wrote down the species that are *known* to exist in nearly equimolar Ni(II)–adenine nucleotide systems. These are, in addition to free metal and ligand ions, the phosphate complex (ML), phosphate-plus-ring complex (ML′), and two possible types of 2:1 complexes, one involving M interacting with ML complex to yield M_2L, the other involving M interacting with ML′ to yield M_2L'. By connecting these species by arrows, we found that the resulting mechanism was completely consistent with the data for both ATP and ADP at all concentrations. The mechanism is the following (A):

$$
\begin{array}{c}
M + ML' \\
[4] \quad \diagdown\diagdown \\
\big\Updownarrow \qquad \diagdown \\
M + L \;\rightleftharpoons\; ML + M \;\rightleftharpoons\; (M_2L, M_2L') \qquad (A) \\
[1] \qquad\qquad [2] \qquad\qquad\quad [3]
\end{array}
$$

The ligand and indicator preequilibria are also included although they are not explicitly written. Solving for the three relaxation times for the above mechanism requires a 3 × 3 determinant,

$$
\begin{vmatrix}
a_{11} + 1/\tau & a_{12} & a_{13} \\
a_{21} & a_{22} + 1/\tau & a_{23} \\
a_{31} & a_{32} & a_{33} + 1/\tau
\end{vmatrix} = 0 \qquad (6)
$$

where

$$
a_{11} = -k_{12}\left(\frac{M}{(1+\beta)} + L + \frac{1}{K_{ML}}\right)
$$

$$
a_{12} = -k_{12}[1/K_{ML}(1+\beta)]
$$

$$
a_{13} = k_{12}\left(L - \frac{1}{K_{ML}}\right)/(1+\beta)
$$

Table IV. Summary of Rate Constants Data for the Interaction of Nickel with Di- and Triphosphates at 15 °C, 0.1 M KNO_3. Previously Determined Values in Parentheses

		Diphosphates			Triphosphates		
		Ni–ADP	Ni–CDP	$NiHP_2O_7$	Ni–ATP	Ni–CTP	$NiHP_3O_{10}$
1:1 Complex							
	Phosphate binding k_{12}, $M^{-1}\,s^{-1}$	5.2×10^5	5.7×10^5	5.3×10^5	1.4×10^6 $(4.1 \times 10^6)^b$	1.3×10^6	1.4×10^6
	k_{21}, s^{-1} ^{a}	170	180	170	55	51	55
	k_{1p}, s^{-1} (calcd)^c	1.6×10^4	1.7×10^4	1.6×10^4	1.7×10^4	1.6×10^4	1.7×10^4
	Back-bound complex						
	k_{24}, s^{-1}	450			1000		
	k_{42}, s^{-1}	120			700		
2:1 Complex							
	K_{M_2L}, $K_{M_2L'}$ (calcd)^d	40	40		160	160	
	k_{23}, $M^{-1}\,s^{-1}$	3.2×10^4	3.2×10^4		1.4×10^5	1.4×10^5	
	k_{32}, s^{-1}	800	800		875	875	
	k_{1p}, s^{-1} (calcd)^e	1.6×10^4	1.6×10^4		1.6×10^4	1.6×10^4	
	k_{43}, $M^{-1}\,s^{-1}$ ^{f}	$\sim 3 \times 10^4$			$\sim 6 \times 10^4$		

^{a} Phosphate dissociation rate constant; the intercept in Figures 4 and 5 is $k_{21}/(1 + K_{24})$. ^{b} At 25 °C and $I = 0.1$ M TMACl; ref 6. ^{c} Calculated from eq 9 with $K_{os}' = 34$ and 80 for the di- and triphosphates, respectively. ^{d} As obtained from the kinetic analysis; see Table II for spectrally measured values. ^{e} Calculated from eq 9 with $K_{os}' = 2$ and 8.7 for the di- and triphosphates, respectively. ^{f} Found for ADP and ATP only; values very approximate; see text.

$$a_{21} = -k_{24}(1 + \beta) - k_{43}[ML'(1 + \beta)] \quad (7)$$

$$a_{22} = -k_{24}(1 + 1/K_{ML'}) - k_{43}M$$

$$a_{23} = k_{24} + k_{43}(ML' + 1/K_{M_2L'})$$

$$a_{31} = k_{43}(ML')(1 + \beta) + k_{23}(1 + \beta)(ML - M)$$

$$a_{32} = (k_{43} - k_{23})(M)$$

$$a_{33} = -k_{43}(ML' + 1/K_{M_2L'}) - k_{23}\left[(ML + M)\frac{1}{K_{M_2L}}\right]$$

and $\beta = H/[K_{a2} + L/(1 + \alpha)]$, $\alpha = In/(K_{In} + H)$.

The three roots have the properties displayed in Figure 6. Roots 1 and 2, too fast to be seen in the temperature jump time region, have the wrong concentration profiles. The slowest root (3) increases linearly at low concentration and plateaus at high concentrations.

In this mechanism both the back-bound species (ML') and the phosphate bound complex (ML) were allowed to form a 2:1 complex. Setting either k_{43} or k_{23} equal to zero (i.e., disallowing that pathway) did not produce a better fit of the data for either ADP or ATP. In fitting this mechanism we have in principle five variables: k_{12} (ML formation), k_{24} (ML' formation), k_{43} (M_2L' formation), k_{23} (M_2L formation), and the stability constant K_{M_2L}. The situation is in practice considerably simplified by the fact that we have very good estimates of k_{12} and k_{23} from our previous work[14] with nickel and the inorganic phosphates and cytosine nucleotides. In addition, the low-concentration data are most sensitive to variations in k_{12}, and the high-concentration region is more sensitive to the value of k_{23}. As a consequence we could independently test the effect of large variations in both rate constants. We found that the best fit for k_{12} and k_{23} was still within the range set by the inorganic phosphates and the cytosine nucleotides (see Table IV). We found that a best fit analysis resulted in k_{43} being comparable to k_{23}; this is reasonable, since pathways 4 → 3 and 2 → 3 both involve formation of a 2:1 complex. The fit was not particularly sensitive to the value of k_{43} over rather wide limits (±50%).

As $f(C) \rightarrow 0$, eq 6 can be shown to have the limiting form

$$\frac{1}{\tau} \simeq k_{12}f(C) + \frac{k_{21}}{1 + K_{24}} \quad (8)$$

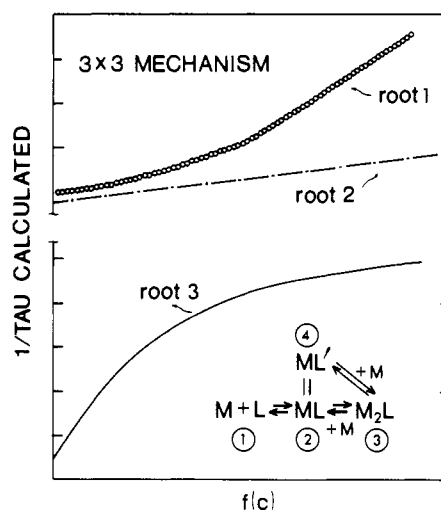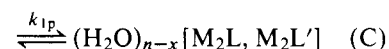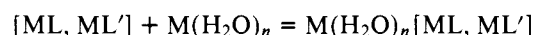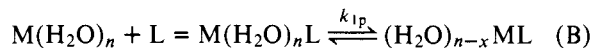That is, the value of k_{12} is in principle obtainable from the

Figure 6. Variation of the three roots ($1/\tau$ values) of eq 6 with $f(C)$.

limiting slopes of Figures 4 and 5. The intercepts, as one would expect, are given by the phosphate dissociation rate constant (k_{21}) divided by $1 + K_{24}$. Thus, the slope to intercept ratio returns the measured stability constant for the 1:1 complexes. It is the presence of the ML' complex that causes the reduction in the intercepts for the adenine nucleotides.

Discussion

In this paper we are concerned with dynamics of the formation of several different metal–nucleotide complexes. The complexation mechanisms for the formation of 1:1 and 2:1 species are more completely described as follows:

$$M(H_2O)_n + L = M(H_2O)_nL \xrightleftharpoons{k_{1p}} (H_2O)_{n-x}ML \quad (B)$$

$$[ML, ML'] + M(H_2O)_n = M(H_2O)_n[ML, ML']$$

$$\xrightleftharpoons{k_{1p}} (H_2O)_{n-x}[M_2L, M_2L'] \quad (C)$$

where n = number of water molecules in the primary hydration sheath of the metal ion and x = the number of water molecules expelled upon reaction.[23] If there is no steric hindrance from the ligand, the forward rate constants for reactions B and C

should be simply

$$k_f = K_{os}'k_{lp} \tag{9}$$

where K_{os}' is the outer-sphere complex association constant (in the medium of 0.1 M KNO_3) and k_{lp} is the ligand penetration rate constant for nickel. For a dissociative mechanism, k_{lp} will very nearly equal the water exchange rate constant k_{H_2O} for the metal ion under study. For nickel at 15 °C, one may estimate k_{H_2O} to be 1.6×10^4 s^{-1}.[24]

The values used for K_{os}' for various charge types are listed in Table IV. This table also contains the rate constants for the complexation of nickel with CDP, CTP, HP_2O_7, and HP_3O_{10} as determined in the preceding paper.[14] One can thus see at a glance the influence of the adenine ring on the formation of the various 1:1 and 2:1 complexes. There follows a discussion of the kinetic results for the various individual steps.

Formation of ML. The rate constant k_{12} equals 5.2×10^5 and 1.4×10^6 M^{-1} s^{-1} for NiADP and NiATP, respectively. Computed values of $k_{lp} \sim 1.6 \times 10^4$ s^{-1} are compatible with the water exchange rate for nickel. In addition, these forward rate constants are identical with the corresponding rate constants for the inorganic phosphates and the cytosine nucleotides. Thus the formation of a phosphate coordinated complex reflects only the charge on the ligand and the exchange rate of the metal ion. There is no sensitivity to the nature of the nucleotide ring, or for that matter to the presence or absence of the entire nucleotide moiety.

The reverse rate constant k_{21} is a measure of the strength of the complex formed. The dissociation rate constants for ML (phosphate binding only) are identical within charge type for the di- and triphosphates. Thus a metal ion bound to *only* the phosphate backbone experiences no steric restriction to its departure when a purine or pyrimidine ring is present in the same molecule. As might be expected, the metal ion dissociates nearly three times more slowly from the triphosphates (three coordination sites) as from the diphosphates (two sites).

Formation of M_2L, M_2L'. Unfortunately we cannot regard the values obtained for k_{23} and k_{43} as unique "best fit" constants for the mechanism. As outlined in the Results section, we have a rather large range of values that can fit the overall mechanism when both ML and ML' are allowed to form a 2:1 complex. The formation rate constants of 3.2×10^4 M^{-1} s^{-1} for ADP and 1.4×10^5 M^{-1} s^{-1} for ATP are identical with those obtained for CDP and CTP, indicating that the expulsion of water molecules is once again the rate-determining step.

The dissociation rate constants for the metal ion in the 2:1 complex in ADP and ATP are also identical with the values found for the corresponding cytosine nucleotides. In addition, k_{32} and k_{34} show no dependence on the phosphate chain length. The same behavior was found for the M_2L complex in our earlier study of magnesium binding to adenine and cytosine nucleotides. This is thus the second time that we have observed that the binding of the second metal ion requires the presence of a nucleotide moiety, and did not discriminate, at least kinetically, between adenosine and cytidine. In the magnesium case, however, the dissociation rate constant k_{32} was 10^4 s^{-1} as opposed to $\sim 10^3$ s^{-1} for the nickel systems.

Formation of ML'. We are faced with a more complicated situation in discussing the formation of the back-bound complex, ML'. In the first place, this species was not found to be present in any other metal-nucleotide system we have studied to date, so we have no other data on the rate of formation of such an intramolecular complex. Second, the structure of a back-bound complex in ATP has been the subject of much debate in the literature since its first proposal by Szent-Gyorgyi in 1957.[25] Some workers favor a complex in which there is a direct bond from the phosphate-bound metal ion to the N_7 position of the adenine ring;[9,10] others postulate a water bridge,[26,27] i.e., hydrogen bond formation from the metal ion

to the N_7 position. This is not a trivial distinction, for the type of binding (inner or outer sphere) could be very important to the biological function of metal-nucleotide complexes. The making and breaking of hydrogen bonds is typically a very rapid process ($\sim 10^9$ s^{-1}).[28] If the binding of the metal ion were through a water bridge, the enzyme system would still see a unique geometry imposed on the ML' complex by the metal ion, but the folded complex could rapidly unfold and make the N_7 site available for further interaction with an enzyme site, substrate, etc. On the other hand, an inner-sphere complex with the metal ion and the ring means that a potentially important ring site could be made accessible only after dissociation of the metal ion. This type of complex would more likely function as an inhibitor, depending, of course, on the requirements of the specific enzymatic reaction.

The rate constants for the formation of ML' are sufficiently small (see Table IV) that they preclude a serious consideration of a water-bridged (outer-sphere) species. This is in agreement with the recent conclusion of Lam et al.,[10] based on a detailed reexamination of the MnATP system, that the back-bound complex involved the N_7 position in a direct (inner sphere) manner. The formation rate constant k_{24} is 450 s^{-1} for NiADP and 10^3 s^{-1} for NiATP. This indicates that it is easier for the phosphate-bound metal ion on the ATP molecule to reach the N_7 position than in ADP. This does not, however, mean that the metal-ATP complex is the more stable. The dissociation rate constant, k_{42}, is 120 s^{-1} for NiADP vs. 700 s^{-1} for NiATP. In NiADP the ring position has to share the positive charge of the metal ion with only two phosphate sites, compared to three in NiATP. Thus, while ML' forms more rapidly in NiATP (presumably because of steric considerations), the back-bound complex in the diphosphate is actually the more stable.

It is interesting to speculate on the possible function(s) of a complex such as ML' in systems utilizing metal bound nucleotides. For both metal ion-nucleotide systems, the species ML' is the predominant 1:1 complex. The presence of a back-bound complex that is unreactive enzymatically would be of more importance as an inhibitor in systems using ADP rather than ATP because of the slower dissociation rate of the former. In addition one would expect Ni^{2+} to generally act as an inhibitor in reaction schemes where an available N_7 site is required. Flagellar motility, for example, involves the enzymatic hydrolysis of ATP. The process is ordinarily activated by divalent metal ions such as Mg^{2+} or Ca^{2+}. Ni^{2+}, on the other hand, is well known to be an effective inhibitor of flagellar motility.[29]

There is a consistent pattern emerging from our series of studies on metal-nucleotide systems—that a multiplicity of metal-nucleotide complexes allows for a variety of regulatory mechanisms by variations in not only the amounts of metal and nucleotide present, but the specific metal and specific nucleotide and complexes thus formed. It is also relevant to point out that only by studying a series of systems with various reactive groups either missing (e.g., inorganic phosphates) or blocked has it been possible to resolve the complicated questions of reaction sites, complexes formed, and rate constants for individual steps.

References and Notes

(1) A preliminary account of this work was presented at the 166th National Meeting of the American Chemical Society, Chicago, Ill., Aug 1973.
(2) NIH Career Development Awardee (17834).
(3) M. Dixon and E. Webb, *Enzymes*, 1, 1 (1964).
(4) W. E. Cleland, *Annu. Rev. Biochem.*, **36**, 77 (1967).

(5) R. M. Izatt, J. J. Christensen, and J. H. Rytting, *Chem. Rev.*, **71**, 439 (1971).
(6) G. G. Hammes and S. A. Levison, *Biochemistry*, **3**, 1504 (1964).
(7) G. G. Hammes and D. L. Miller, *J. Chem. Phys.*, **46**, 1533 (1967).
(8) M. Cohn and T. R. Hughes, *J. Biol. Chem.*, **235** 3250 (1960).
(9) (a) H. Sternlicht, R. G. Shulman, and E. W. Anderson, *J. Chem. Phys.*, **43**, 3123 (1965); (b) *ibid.*, **43**, 3133 (1965).
(10) Y-F. Lam, G. P. P. Kuntz, and G. Kotowycz, *J. Am. Chem. Soc.*, **96**, 1834 (1974).
(11) P. W. Schneider, H. Brintzinger, and H. Erlenmeyer, *Helv. Chim. Acta*, **47**, 992 (1964).
(12) U. Weser, *Struct. Bonding (Berlin)*, **5**, 41 (1968).
(13) C. M. Frey, J. L. Banyasz, and J. E. Stuehr, *J. Am. Chem. Soc.*, **94**, 9198 (1972).
(14) C. M. Frey and J. E. Stuehr, *J. Am. Chem. Soc.*, preceding paper in this issue.
(15) T. A. Glassman, J. Suchy, and C. Cooper, *Biochemistry*, **12**, 2430 (1973).
(16) C. M. Frey and J. E. Stuehr in "Metal Ions in Biological Systems", Vol. 1, H. Sigel, Ed., Marcel Dekker, New York, N.Y., 1974.
(17) C. M. Frey and J. E. Stuehr, *J. Am. Chem. Soc.*, **94**, 8898 (1972).
(18) Glassman et al.[15] have shown that metal–phosphate coordination alone—such as in Ni-gATP [9-(β-D-glucopyranosyl)adenine 6'-triphosphate], where steric restraints forbid the formation of a back-bound complex—does *not* cause a perturbation of the adenine ring spectrum.
(19) J. A. Happe and R. L. Ward, *J. Am. Chem. Soc.*, **91**, 4906 (1969).
(20) R. S. Taylor and H. Diebler, *Bioinorg. Chem.*, **6**, 247 (1976); have recently reported a binding constant of 2 ± 0.6 M^{-1} for the nickel-adenosine complex.
(21) The relaxation amplitude was found to maximize at intermediate concentrations. At the high and low concentration extremes the equilibrium amounts of one or more components decreased, resulting in smaller perturbations.
(22) H. Sternlicht, D. E. Jones, and K. Kustin, *J. Am. Chem. Soc.*, **90**, 7110 (1968).
(23) H. Eigen and K. Tamm, *Z. Elektrochem.*, **66**, 93, 107 (1962).
(24) J. W. Neeley and R. E. Connick, *J. Am. Chem. Soc.*, **94**, 3419 (1972).
(25) A. Szent-Gyorgyi, "Bioenergetics", Academic Press, New York, N.Y., 1957, p 64.
(26) T. A. Glassman, C. Cooper, L. W. Harrison, and T. J. Swift, *Biochemistry*, **10**, 843 (1971).
(27) G. P. P. Kuntz, T. A. Glassman, C. Cooper, and T. J. Swift, *Biochemistry*, **11**, 538 (1972).
(28) G. G. Hammes and A. C. Park, *J. Am. Chem. Soc.*, **91**, 956 (1969); G. G. Hammes and P. J. Lillford, *ibid.*, **92**, 7578 (1970).
(29) N. Flavin and C. Staughter, *J. Bacteriol.*, **118**, 59 (1974).

A Stable Chromium(V) Compound. Synthesis, Properties, and Crystal Structure of Potassium Bis(2-hydroxy-2-methylbutyrato)-oxochromate(V) Monohydrate[1]

Miroslav Krumpolc, Barry G. DeBoer,*[2] and Jan Roček*

Contribution from the Department of Chemistry, University of Illinois at Chicago Circle, Chicago, Illinois 60680. Received August 13, 1976

Abstract: The first stable water-soluble chromium(V) compound, potassium bis(2-hydroxy-2-methylbutyrato)oxochromate(V) monohydrate, $K[OCr(O_2CCOMeEt)_2] \cdot H_2O$, was prepared in crystalline form from chromium trioxide and 2-hydroxy-2-methylbutyric acid; its spectral (UV, ESR, IR) properties and other physical data are given. The stability of the compound is discussed. A bicyclic structure proposed on the basis of the elemental composition and spectral data was confirmed by x-ray diffraction. The compound crystallizes in the noncentrosymmetric monoclinic space group Cc with lattice parameters $a = 12.362$ (6), $b = 16.665$ (9), $c = 7.611$ (3) Å, $\beta = 90.33$ (3)°, $V = 1567.9$ (13) Å^3. For $Z = 4$ and formula weight 357.35, ρ (calcd) = 1.514 g cm^{-3}, ρ (obsd) = 1.518 (5) g cm^{-3}. The 736 data were collected from a small, fractured crystal using an autodiffractometer and Mo Kα radiation (2θ (max) = 40°) and the structure refined to $R(F) = 7.06\%$ and $R(wF) = 6.79\%$. The anion geometry is very similar to those found for isoelectronic VO^{2+} complexes (Cr–O = 1.554 (14) Å) and is intermediate between square pyramidal and trigonal bipyramidal.

The preparation of stable chromium(V) compounds is of considerable importance not only to chemistry, but also to nuclear physics. For many years, chemists have been aware of the crucial role of these intermediates in all known mechanisms[3] of chromium(VI) oxidations. The interest of nuclear physicists stems from the observation that chromium(V) complexes in media of high hydrogen content are among the most efficient paramagnetic species available for the preparation of dynamically polarized proton targets needed in the study of high-energy particle interactions.[4–7]

The first observation indicating the formation of chromium(V) complexes in the course of oxidation of several organic acids (oxalic, lactic, citric) by potassium dichromate in glacial acetic acid was reported by Kon.[8,9] Higher concentrations of relatively more stable chromium(V) complexes were prepared by the reduction of potassium dichromate by glycerol,[10] ethylene glycol,[11,12] dithioethylene glycol,[13] several phenol derivatives,[14] diethylene glycol,[15] and 1,2-propanediol.[16]

None of these studies, however, resulted in isolation of a stable, well-characterized chromium(V) compound. A survey of the literature of pentavalent chromium reveals that relatively few compounds of known composition have been prepared, mostly derivatives of oxo species CrO_4^{3-}, $Cr(O_2)_4^{3-}$, and CrO^{3+}. The anions are known to form hypochromates $M_3^I CrO_4$ (M = Li, Na),[17] $M_3^{II}[(CrO_4)_2]$, $M_5^{II}[(CrO_4)_3OH]$ (M = Ca, Sr, Ba),[18] and peroxides $M_3^I[Cr(O_2)_4]$ (M = NH$_4$, Na, K).[19] Derived from the oxocation CrO^{3+} and the related anions $CrOX_4^-$ and $CrOX_5^{2-}$ (X = F, Cl) are the oxotrichloride $CrOCl_3$,[20] perfluoropinacolates $M^I[CrO(pfp)_2]$ (M = K, Cs, Et$_4$N),[21] fluorooxo complexes $M^I[CrOF_4]$ (M = K, Ag)[22] and $(Et_4N)_2[CrOF_5]$,[23] chlorooxo complexes M^I-$[CrOCl_4]$ (M = Me$_4$N, Et$_4$N, Pr$_4$N, Bu$_4$P, Ph$_4$As, BzPh$_3$P)[23] and $M_2^{II}[CrOCl_5]$ (M = NH$_4$, K, Rb, Cs),[24] and binary salts (the "Weinland complexes") of the types RNH-$[CrOCl_4]$,[20,25,26] $[RNCOR][CrOCl_4]$,[20] and $[NHRNH]$-$[CrOCl_5]$[20] with nitrogen bases (pyridine, quinoline, o-phenanthroline, etc.). Other chromium(V) compounds reported in the literature are the oxide Cr_2O_5,[27] the fluoride CrF_5,[28] dibenzoatotrichlorochromium(V)[20] $(C_6H_5CO_2)$-$_2CrCl_3$, and the chlorooxo complexes $Cs_2[CrO(AB)Cl_3]$ (AB = anions of tartaric, hydroxymalonic, and malic acids).[23] All these compounds (except peroxides[29] and perfluoropinacolates, which are insoluble in water[21]) are characterized by their high instability with respect to hydrolytic decomposition. Although